ARPES view of low energy electronic interactions in superconducting cuprates

A.A. Kordyuk and S.V. Borisenko
Institute for Solid State Research, IFW-Dresden, Helmholtzstr. 20, D-01069 Dresden, Germany
Institute of Metal Physics of National Academy of Sciences of Ukraine, 03142 Kyiv, Ukraine

While the pronounced doping dependence of the quasiparticle spectral weight in the antinodal region of the superconducting cuprates, as seen by ARPES, unambiguously points to the magnetic origin of the strong electron-boson coupling there, the nature of the electron scattering in the nodal direction remained unclear. Here we present a short review of our recent detailed investigations of the nodal direction of Bi-2212. Our findings prove the existence of well defined quasiparticles even in the pseudogap state and show that the essential part of the quasiparticle scattering rate, which appears on top of Auger-like electron-electron interaction, also implies a magnetic origin.

Angle-resolved photoemission spectroscopy (ARPES) [1] provides a direct view on the density of low energy electronic excited states in solids—the 2D detector of the electron analyzers used in modern ARPES is just a window into momentum-energy space of 2D solids. A snapshot through this window stores the quasiparticle spectral weight in the momentum-energy co-ordinates [2-5]. Being essentially two-dimensional, the superconducting cuprates are a perfect example of the arpesable compounds [1]. All the interactions of the electrons which are responsible for their unusual normal and superconducting properties are encapsulated in such snapshots, and success in understanding of the nature of electronic interactions in the cuprates depends, in the first place, on how clear the ARPES window is. Then, the experimental experience (namely, how many different snapshots have been taken and made out) comes into play. But taking into account a number of parameters (e.g. temperature and doping) which cause a redistribution of the quasiparticle spectral weight, the detailed exploration of the momentum-energy space, even for one compound, will take ages of experimental work.

Leaving such a global task for the nearest future, one can focus on the two cuts in the Brillouin zone (BZ), nodal and antinodal directions (see Fig. 1a). These regions represent an inherent anisotropy of the electronic interactions in the cuprates which appear in anisotropy of the superconducting gap [6], pseudo-gap [7], and coupling strength [8] (or scattering in general). While the pronounced doping dependence of the quasiparticle spectral weight in the antinodal region of the BZ unambiguously points out to the magnetic origin of the strong electron-boson coupling seen by ARPES [9-11] (see Fig. 1 c-f), the nature of the electron scattering in the nodal direction remained unclear. Here we review the results of a detailed investigation of the nodal direction of Bi-2212 in a wide range of doping, temperature and excitation energy. We have found that although the electronic band structure along the nodal direction remains complex due to non-vanishing bilayer splitting, the quasiparticle spectral weight distribution from each split band can be self-consistently described within the quasiparticle self-energy approach. The scattering rate, on the other hand, can be considered as a sum of two main channels: the doping independent channel can be well understood in terms of the conventional Fermi liquid model, while the additional doping dependent channel implies a magnetic origin.

Experimental cornerstones. The experimental details can be found elsewhere [5, 9, 10], but here we highlight the cornerstones which are peculiar to our experiments. They are: the precise cryo manipulator, the wide excitation energy range, and the superstructure-free samples.

The precise cryo manipulator operates in the controlled temperature range from 20 K to 400 K and allows us to translate the sample in three perpendicular directions and rotate it around three perpendicular axes in steps of 0.1º, that secures the precise positioning and easy motion of the ARPES window in the momentum space.

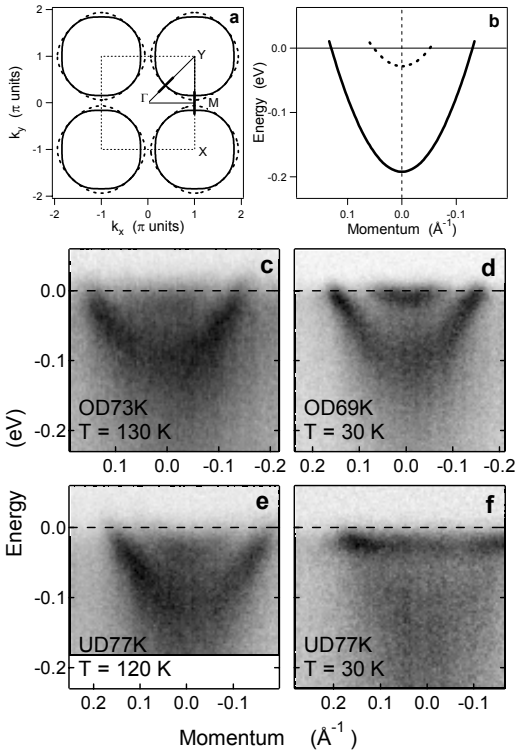

Fig. 1. Electronic band structure of an overdoped Bi-2212 [6]: Fermi surfaces (a) and the "XMY" cut (b). ARPES snapshots taken along the XMY direction of the BZ [10] for the overdoped (c, d) and underdoped (e, f) samples above (c, e) and below (d, f) T_c.

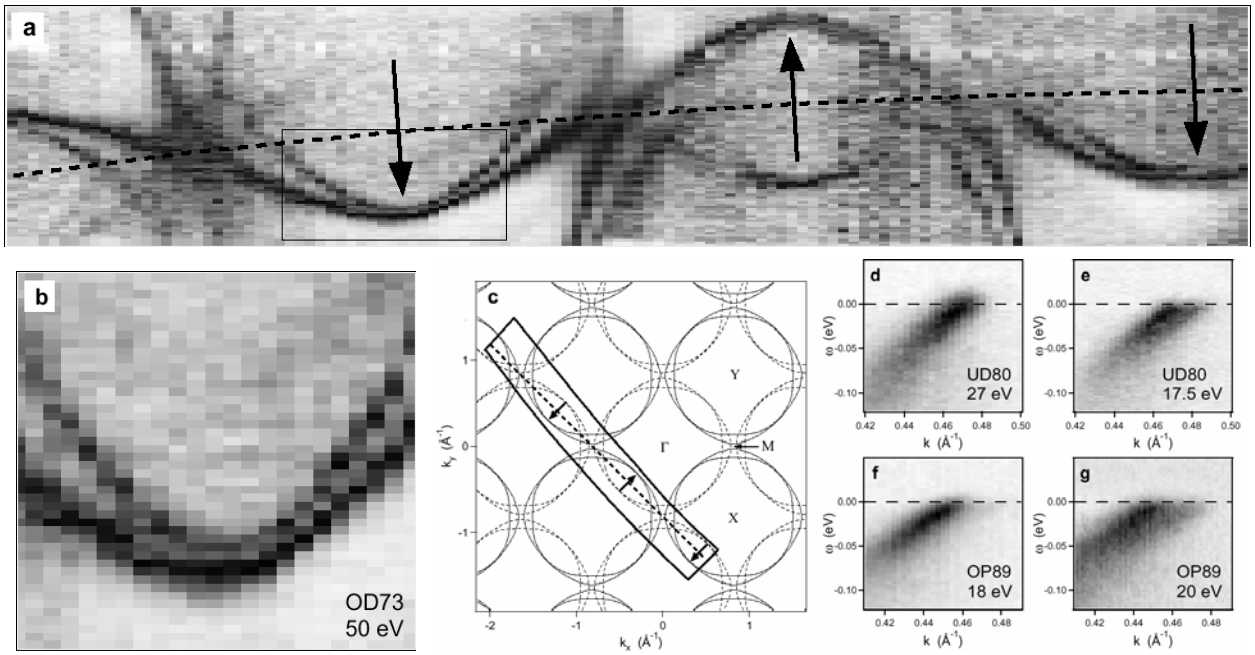

The photons of different energy and polarization have appeared to be an extremely useful tool to selectively excite the electrons from different bands [12, 13]. As a light source we use a He discharge lamp, linearly polarized light from a high resolution beamline (U125/1-PGM at BESSY) with a wide excitation energy range (17–600 eV), or circularly polarized light (4.2R beamline "Circular Polarization" at ELETTRA).

The well known problem for ARPES on Bi-2212 is a "5x1" superstructure which produces a number of diffraction replicas along the BZ diagonal (ΓY direction) [14, 15]. This highly complicates the analysis of the spectra taken from certain areas of the BZ (e.g., the antinodal region [12, 16]) or, if the main features and replicas are spatially separated (e.g. along ΓY direction), reduces the photocurrent intensity. Another important point about Bi-2212 samples, which becomes crucial now [17, 18], is that one needs to know precisely their doping level. We studied both the led-doped superstructure-free Bi(Pb)-2212 and reach of replicas pure Bi-2212. However, as the main line, we use the well characterized superstructure-free samples of a wide doping range (x = 0.11 – 0.22), for which the charge carrier densities have been derived from the measured Fermi-surface area (and appeared to be consistent with their T_c) [19] and the tight-binding parameters have been determined [6]. The parameters of the band structure of the pure Bi-2212 samples which we have measured are also in agreement with their doping level estimated from the T_c measurements.

Fig. 2. Experimental evidence for nodal splitting. (a) Fermi surface map of Bi(Pb)-2212 OD73 measured with 50 eV excitation energy at 25 K over a wide momentum region shown in (c): pointing up and down arrows mark the nodal directions in the 1st and 2nd Brillouin zone (BZ) respectively; the area of interest within the rectangle in (a) is zoomed in in (b); the dashed line goes through M-points representing the boundary of the "magnetic" BZ. (d-g) A set of images of the energy distribution maps (EDMs) for Bi-2212 UD80 (d,e) and Bi-2212 OP89 (f,g) measured at 25 K along different nodal directions at different excitation energy: (d) and (e) in the 1st BZ along the (0,0)–(π,–π) direction, (f) and (g) in the 2nd BZ in (2π,0)–(π,π) direction.

Complex structure. A distinguishing feature of modern ARPES is the ability to resolve the bilayer splitting (BS) of the CuO conduction band in the bilayer cuprates. For the first time such a splitting has been observed for overdoped Bi-2212 [20, 21] and then also for optimally doped and underdoped samples [19, 22] (clearly resolved below [19, 23] and above [10] the superconducting transition, as one can see in Fig. 1 c-e). It has been found [20, 21] that the observed splitting can be approximated by a momentum dependence: $t_\perp (\cos k_x - \cos k_y)^2/2$, which is expected for an inter-plane hopping between two CuO layers (where $t_\perp$ describes the interlayer hopping mainly mediated via Cu4*s* orbitals). The splitting along the node is expected to be much less than the maximum splitting at the saddle-point [24] but has been never observed.

Recently, we have resolved the nodal splitting for a number of Bi-2212 samples of different doping level [25]. Fig. 2 illustrates this.

Simple physics. Apparently, the nodal splitting found in Bi-2212, if not taken into account, can intricately complicate the nodal spectra. Even if unresolved, it should influence the quantities derived from these spectra, e.g. the renormalized dispersion or scattering rate. It is observed as a dependence of these quantities on excitation energy. In the following we try to eliminate the influence of the splitting choosing an appropriate excitation energy. We focus on the experimental dataset taken at 27 eV in order to find out whether the quasiparticle spectral weight from only one band can be

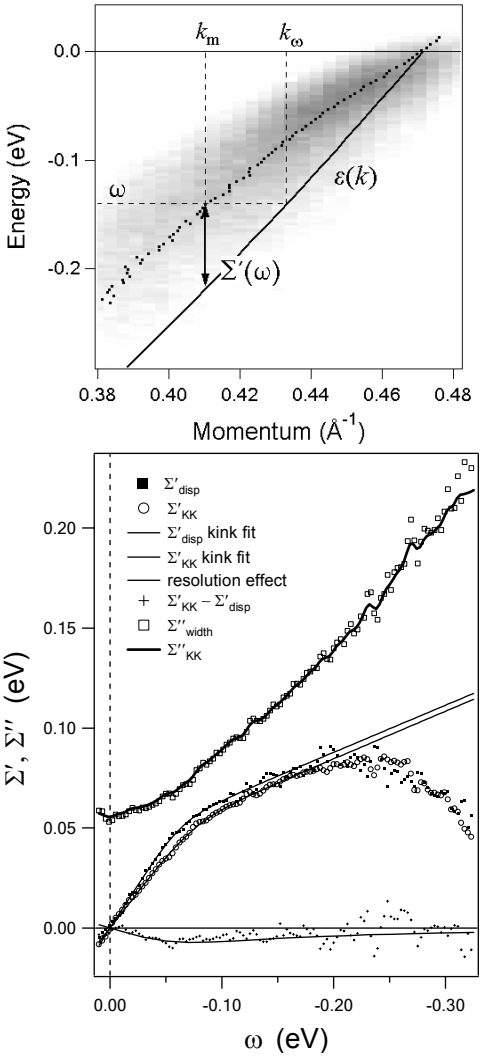

described by "simple physics", i.e. in terms of quasiparticle self-energy [26].

Fig. 3 (top) illustrates the basics of the nodal spectra analysis within the self-energy approach [27, 28]. The black solid line represents a non-interacting case when the spectral function is a delta function with the pole $\omega - \varepsilon(\mathbf{k}_\omega) = 0$, $\varepsilon(\mathbf{k})$ is called "bare dispersion". A simple electronic interaction leads to shifting and broadening of the non-interacting spectral function and the resulting picture is essentially that which is measured by ARPES: the blurred region in Fig. 3 illustrates the distribution of the quasiparticle spectral weight. Such an interaction can be described by introducing a quasiparticle self-energy $\Sigma = \Sigma' + i\Sigma''$, an analytical function the real and imaginary parts of which are related by the Kramers-Kronig (KK) transformation [29]. Neglecting the momentum dependence of the self-energy, the MDC at certain ω exhibits a Lorentzian lineshape [4] with the maximum at $k_m(\omega)$ determined by $\Sigma'(\omega) = \omega - \varepsilon(k_m)$, which is illustrated in Fig. 3 by the double headed arrow (squared symbols show the renormalized dispersion). In the region where the bare dispersion can be considered as linear ($\varepsilon = v_F k$), the MDC width W (the half width at half maximum) is proportional to Σ": $\Sigma''(\omega) = -v_F W(\omega)$. Thus, the determination of both the real and imaginary parts of the self-energy requires the knowledge of the bare dispersion. The KK transformation, giving an additional equation to relate these functions, opens the way to extract all desired quantities from the experiment (see [27, 28] for the details). Fig. 3 (bottom) shows the results for an underdoped Bi(Pb)-2212 (T_c = 77 K) at 130 K, i.e. in the pseudo-gap state. Σ'(ω) calculated in two ways have appeared to be identical for the certain v_F = 3.82 ± 0.17 eVÅ. This gives the following interaction parameters: λ = 0.87 ± 0.12, Z = 0.54 ± 0.03. The extracted bare band dispersion is in good agreement with the band structure calculations [25] and allows one to quantify the self-energy of the electronic excitations on the real energy scale.

Fig. 3. Bare band dispersion (solid line) and renormalized dispersion (symbols) on top of the spectral weight of interacting electrons (top). Real and imaginary parts of the self-energy extracted from the experiment with the described procedure (bottom). A complete coincidence between the corresponding parts of the self-energy calculated from the two different experimental functions, the MDC dispersion and MDC width, demonstrates the full self-consistency of the ARPES data treated within the self-energy approach.

The demonstrated self-consistency can be considered as a validity criterion for photoemission spectra, since it weeds out not only a "complex structure" like splitting or admixture of other bands but also artificial effects like inhomogeneity of the detector, etc. Considering the intimate relation between Σ' and Σ" one can distinguish two energy scales in Fig. 3. One, at about 200 meV, corresponds to the maximum of Σ'(ω) and is related to the cut-off energy for Σ"(ω). Another, at 70 meV, is a famous "kink", it develops as a sharp bend between two linear segments of Σ'(ω), is related to the "drop" in the scattering rate [30-32], and commonly explained as an interaction with a bosonic mode [3, 4]. It is important to distinguish these two scales in order to find out the nature of the coupling boson.

As far as the kink on the dispersion appears as just a sharpening of a bend of the same sign in the experimental dispersion which is present at every temperature and doping [30, 33], we focus on the "scattering rate kink" [32] which is much more convenient in this sense because it develops on top of the strong normal state scattering of the opposite curvature. Studying a number of samples of different doping level at different temperature we have found that the scattering rate kink makes it possible to distinguish between the different scattering channels [32]. We argue that the main contribution to the scattering can be well understood in terms of the conventional Fermi liquid model (FL) [26] while the additional doping dependent contribution apparently has a magnetic origin.

Fig. 4a shows the scattering rate (in momentum units) as a function of frequency for optimally doped Bi(Pb)-2212 OP89 for different temperatures. A sharp kink seen in Σ"(ω) at 0.1 eV (indicated by the arrow) at 40 K (below T_c = 88 K) gradually vanishes with increasing temperature. Another important finding is that

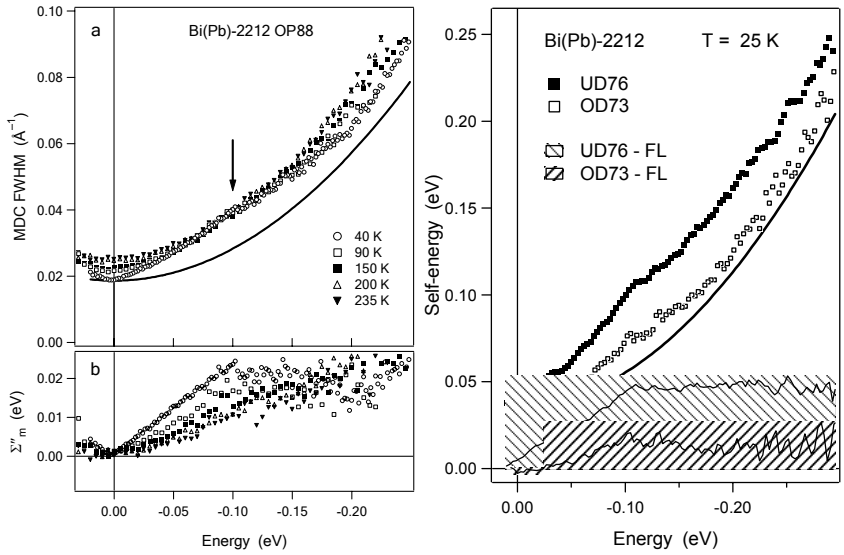

Fig. 4. (a) Temperature dependence of the scattering rate for the nodal quasiparticles in optimally doped Bi(Pb)-2212. The solid line represents a contribution from the usual Auger decay (Fermi liquid parabola) obtained by fitting the data for highly overdoped sample (OD69) at 130 K. (b) Result of a subtraction of the Fermi liquid parabola for each temperature in terms of the imaginary part of the self-energy (the FWHM/2 is multiplied to the bare Fermi velocity v_F = 4 eVÅ). (c) Strengthening of the scattering mode with underdoping. Comparison of the imaginary part of the self-energy of nodal quasiparticles in Bi(Pb)-2212 underdoped (T_c = 76 K) and overdoped (T_c = 73 K) samples at 25 K. The shaded areas represent the contributions from the magnetic scattering obtained by subtraction of the FL parabola [32].

the high binding energy tail of $\Sigma''(\omega)$ shifts upwards with temperature similar to the $\Sigma''(0)$ value. This shift, being in agreement with optical conductivity results [34], contradicts, in fact, the marginal FL scenario [35], according to which $\Sigma''(\omega, T) \sim \max(|\omega|, T)$. Such a shift of the whole curve is expected within the FL model when the scattering rate is determined by an Auger-like decay (the process where the hole decays into two holes and one electron [26]) that gives $\Sigma'' \sim \omega^2 + (\pi T)^2$. The FL behavior is generally expected for overdoped samples [36], and in Fig. 4a we add the FL parabola (solid line) which perfectly fits the scattering rate for an OD69 sample above T_c in the whole binding energy range. This parabola evidently describes the main contribution to Σ'' at any temperature. The additional contribution, which is seen as a hump on top of the FL parabola, must originate from an additional interaction which can be responsible for the unusual properties of the cuprates. In Fig. 4b we evaluate this interaction subtracting the FL parabola for each temperature and setting the resulting offsets to zero.

Therefore, this additional contribution decreases with increasing temperature, and we have found that it vanishes above T_c for the overdoped samples, but persists at higher temperatures, presumably up to T^* for optimally doped and underdoped samples [32]. In Fig. 4c we compare the absolute values of $\Sigma''(\omega)$ for underdoped (UD76) and overdoped (OD73) Bi(Pb)-2212 at T = 25 K. The room temperature scattering rates for these two samples coincide within the experimental error bars. It is seen that at low temperature the underdoped sample exhibits a much higher scattering rate with a more pronounced kink that has a tendency to disappear completely at higher doping levels [30]. The differences between these data and the FL parabola (solid line, the same as in Fig. 4a) demonstrate that the additional scattering channel of the nodal quasiparticles is highly doping dependent which is difficult to reconcile with the phonon scenario [31, 37], leaving space for magnetic excitations as the only bosons responsible for this additional channel [38, 39].

1. For review see A. Damascelli, Z. Hussain, and Z.-X. Shen, Rev. Mod. Phys. 75, 473 (2003).
2. T. Valla et al., Science 285, 2110 (1999).
3. P. V. Bogdanov et al., Phys. Rev. Lett. 85, 2581 (2000).
4. A. Kaminski et al., Phys. Rev. Lett. 86, 1070 (2001).
5. S. V. Borisenko et al., Phys. Rev. B 64, 094513 (2001).
6. A. A. Kordyuk et al., Phys. Rev. B 67, 064504 (2003).
7. Z.-X. Shen et al., Phys. Rev. Lett. 70, 1553 (1993).
8. H. Ding et al., Nature 382, 51 (1996).
9. T. K. Kim et al., Phys. Rev. Lett. 91, 167002 (2003).
10. S. V. Borisenko et al., Phys. Rev. Lett. 90, 207001 (2003).
11. A. D. Gromko et al., Phys. Rev. B 68, 174520 (2003).
12. A. A. Kordyuk et al., Phys. Rev. Lett. 89, 077003 (2002).
13. S. V. Borisenko et al., Phys. Rev. B 69, 224509 (2004).
14. H. Ding et al., Phys. Rev. Lett. 76, 1533 (1996).
15. S. V. Borisenko et al., Phys. Rev. Lett. 84, 4453 (2000).
16. S. V. Borisenko et al., Phys. Rev. Lett. 92, 207001 (2004); S. V. Borisenko et al., Nature 431, U1 (2004).
17. J. Hwang et al., Nature 427, 714 (2004); T. Valla et al., cond-mat/0405203.
18. T. Cuk et al., cond-mat/0403743.
19. A. A. Kordyuk et al., Phys. Rev. B 66, 014502 (2002).
20. D. L. Feng et al., Phys. Rev. Lett. 86, 5550 (2001).
21. Y.-D. Chuang et al., Phys. Rev. Lett. 87, 117002 (2001).
22. Y.-D. Chuang et al., cond-mat/0107002.
23. S. V. Borisenko et al., Phys. Rev. B 66, 140509 (2002).
24. O. K. Andersen et al., J. Phys. Chem. Solids 56, 1573 (1995).
25. A. A. Kordyuk et al., cond-mat/0311137.
26. A. A. Abrikosov, L. P. Gor'kov, and I. E. Dzyaloshinskii Quantum Field Theoretical Methods in Statistical Physics (Pergamon, Oxford), (1965).
27. A. A. Kordyuk et al., cond-mat/0405696.
28. A. A. Kordyuk et al., cond-mat/0409483.
29. L. D. Landau and E. M. Lifschitz, Statistical Physics, Part 1 (Pergamon, Oxford, 1980).
30. A. Koitzsch et al., Phys. Rev. B 69, 140507 (2004).
31. X. J. Zhou et al., Nature 423, 398 (2003).
32. A. A. Kordyuk et al., Phys. Rev. Lett. 92, 257006 (2004).
33. P. D. Johnson et al., Phys. Rev. Lett. 87, 177007 (2001).
34. D. van der Marel et al., Nature 425, 271 (2003).
35. C. M. Varma, et al., Phys. Rev. Lett. 63, 1996 (1989).
36. C. M. Varma, et al., Phys. Rep. 361, 267 (2002).
37. A. Lanzara et al., Nature 412, 510 (2001).
38. H. F. Fong et al., Phys. Rev. B 61, 14773 (2000).
39. M. Eschrig and M. R. Norman, Phys. Rev. B 67, 144503 (2003).